

Apolipoprotein E ϵ 4 is associated with disease-specific effects on brain atrophy in Alzheimer's disease and frontotemporal dementia

Federica Agosta^{a,b,1}, Keith A. Vossel^{a,1}, Bruce L. Miller^a, Raffaella Migliaccio^{a,c}, Stephen J. Bonasera^a, Massimo Filippi^b, Adam L. Boxer^a, Anna Karydas^a, Katherine L. Possin^a, and Maria Luisa Gorno-Tempini^{a,2}

^aMemory and Aging Center, Department of Neurology, University of California, 350 Parnassus Avenue, Suite 905, San Francisco, CA 94143; ^bNeuroimaging Research Unit, Scientific Institute and University Hospital San Raffaele, via Olgettina 60, 20132 Milan, Italy; and ^cDepartment of Neurological Sciences, II University of Naples, Piazza Miraglia, 80738 Naples, Italy

Communicated by Robert Mahley, The J. David Gladstone Institutes, San Francisco, CA, December 13, 2008 (received for review July 31, 2008)

Apolipoprotein ϵ 4 (apoE4) has been strongly linked with Alzheimer's disease (AD) and contributes to several other neurological disorders. We investigated the influence of ϵ 4 allele carrier status on the pattern of gray matter atrophy and disease severity in 51 patients with probable AD and 31 patients with behavioral variant frontotemporal dementia (bvFTD), compared with 56 healthy controls. Voxel-based morphometry was performed by using statistical parametric mapping. The ϵ 4 allele frequency was higher in the AD group ($P < 0.001$) than the controls but not in the bvFTD group. No differences in demographic or cognitive profiles were observed between ϵ 4 allele carriers and noncarriers within any of the diagnostic groups. However, ϵ 4 carrier status was associated with more severe brain atrophy in disease-specific regions compared with noncarriers in both AD and bvFTD. AD ϵ 4 carriers showed greater atrophy in the bilateral parietal cortex and right hippocampus, and bvFTD ϵ 4 carriers demonstrated greater atrophy in the bilateral medial, dorsolateral, and orbital frontal cortex, anterior insula, and cingulate cortex with right predominance. This regional ϵ 4 effect is consistent with the hypothesis that apoE may affect the morphologic expression uniquely in different neurodegenerative diseases. The atrophy patterns in ϵ 4 carriers may indicate that they are at greater risk for clinical progression.

AD/FTD | apoE | brain morphometry

The apolipoprotein E (apoE) gene is localized on chromosome 19 in a single locus with three alleles (ϵ 2, ϵ 3, and ϵ 4) responsible for the three major apoE isoforms (apoE2, apoE3, and apoE4) (1). Through its function in lipid transport and cellular metabolism, apoE plays a fundamental role in cell maintenance and repair (2). However, in the CNS, apoE2 and E3 are more effective in this role than apoE4, and apoE4 may be detrimental in the process (1).

Possessing at least one ϵ 4 allele is the major known genetic risk factor yet identified for sporadic Alzheimer's disease (AD), with a dose-dependent effect on age of onset (3) and rate of cognitive decline (4). ApoE ϵ 4 allele carrier status has been associated with subtle impairments in cognition in "normal" individuals including poorer verbal episodic memory (5). In addition, apoE4 may influence disease onset, risk, progression, or outcome in number of other neurological conditions including traumatic brain injury (6), aneurysmal subarachnoid hemorrhage (7), cerebral amyloid angiopathy (8), Parkinson's disease (9), dementia with Lewy bodies (10), and ALS (11).

The mechanisms underlying the role of apoE4 in AD and other neurological disorders are still poorly understood. Emerging data suggest that apoE4 contributes to neurological disease through multiple pathways (1). In animal models of AD, apoE4 increases amyloid β (A β) deposition and impairs its clearance leading to plaque formation (12) and enhances lysosomal leakage (13). Also, in AD patients, apoE4 is associated with a higher density of amyloid plaques (14). ApoE4 may also act indepen-

dently of the A β peptide through dysregulation of tau phosphorylation, disruption of cytoskeletal structure, and mitochondrial damage. In neurons that are uniquely vulnerable to injury in neurodegenerative diseases, apoE4 may exacerbate existing pathology (1).

Whether apoE4 may be a genetic disease modifier in frontotemporal lobar degeneration (FTLD) remains poorly understood. Studies on the effect of apoE4 on FTLD have yielded contradictory results (15–18), which likely reflects the complex clinical, pathological, and genetic underpinnings of this disease. The only prospective study that has investigated the effect of apoE genotype on clinical expression in frontotemporal dementia (FTD) revealed an ϵ 4 dose-dependent influence on behavioral symptoms in behavioral variant frontotemporal dementia (bvFTD) (18).

Neuroimaging studies mapping brain structural changes associated with apoE in AD have shown an ϵ 4 allele dose-effect on hippocampal, amygdalar, and entorhinal cortical atrophy (19–21). To our knowledge, only one small case series investigated the apoE4 morphologic effect in bvFTD, showing a trend of greater right frontal lobar atrophy in patients carrying the ϵ 4 allele (21).

In this study, we performed a clinical and voxel-based morphometry (VBM) analysis to investigate the influence of apoE ϵ 4 allele carrier status on disease severity and gray matter (GM) atrophy in a large cohort of patients with probable AD and bvFTD at presentation. VBM is an unbiased neuroimaging technique for the detection of regional brain atrophy by voxel-wise comparison of GM volume between groups of subjects, and it has been shown to be sensitive in detecting specific regions of GM atrophy in neurodegenerative diseases (22). Based on current hypotheses regarding the role of apoE4 on the pathogenesis of neurodegenerative disease, we hypothesized that apoE4 would show different, disease-specific effects in both AD and bvFTD.

Results

Genetic, Demographic, Clinical and Cognitive Data. ApoE genotype and allele frequencies for all subjects are given in Table 1. ApoE ϵ 4 carriers (possessing at least one ϵ 4 allele) were 30 (58.8%) within the AD group, eight (25.8%) within the bvFTD group,

Author contributions: F.A., K.A.V., B.L.M., and M.L.G.-T. designed research; F.A., K.A.V., and M.L.G.-T. performed research; S.J.B., A.L.B., and A.K. contributed new reagents/analytic tools; F.A., K.A.V., R.M., S.J.B., A.L.B., A.K., K.L.P., and M.L.G.-T. analyzed data; and F.A., K.A.V., B.L.M., M.F., and M.L.G.-T. wrote the paper.

The authors declare no conflict of interest.

¹F.A. and K.A.V. contributed equally to this work.

²To whom correspondence should be addressed. E-mail: marilu@memory.ucsf.edu.

This article contains supporting information online at www.pnas.org/cgi/content/full/0812697106/DCSupplemental.

© 2009 by The National Academy of Sciences of the USA

Table 1. ApoE genotype and allele frequencies for patients with AD, bvFTD, and healthy controls

Subjects	ApoE genotype						Allele frequency, %			
	$\epsilon 2/\epsilon 2$	$\epsilon 2/\epsilon 3$	$\epsilon 2/\epsilon 4$	$\epsilon 3/\epsilon 3$	$\epsilon 3/\epsilon 4$	$\epsilon 4/\epsilon 4$	$\epsilon 2$	$\epsilon 3$	$\epsilon 4$	$\epsilon 4$ carriers, %
AD (51 subjects)	0	1*	0	20*	26**	4**	1.0*	65.7	33.3**	58.8
bvFTD (31 subjects)	0	3	0	20	8	0	4.8	82.3	12.9	25.8
Controls (56 subjects)	1	10	2	35	8	0	12.5	78.6	8.9	17.9

Differences among the groups in apoE genotypes and allele frequencies were tested by using the Pearson χ^2 test.

*Significantly lower than controls ($P < 0.05$).

**Significantly higher than controls ($P < 0.05$).

and 10 (17.9%) within the control group. In the AD group, the frequencies of the $\epsilon 2/\epsilon 3$ and $\epsilon 3/\epsilon 3$ genotypes were lower than in the control group [$\epsilon 2/\epsilon 3$: $\chi^2 = 7.3$, $P = 0.007$, likelihood ratio (LR) 8.5; $\epsilon 3/\epsilon 3$: $\chi^2 = 5.8$, $P = 0.016$, LR 5.8] and the frequencies of the $\epsilon 3/\epsilon 4$ and $\epsilon 4/\epsilon 4$ genotypes were higher than the control group ($\epsilon 3/\epsilon 4$: $\chi^2 = 16.6$, $P < 0.001$, LR 17.2; $\epsilon 4/\epsilon 4$: $\chi^2 = 4.6$, $P = 0.033$, LR 6.1). Also, in the AD group, the frequency of the $\epsilon 3/\epsilon 3$ genotype was lower than in the bvFTD group ($\chi^2 = 4.9$, $P = 0.026$, LR 5.0). No significant differences in genotype frequencies were found between bvFTD and controls. In the AD group, the $\epsilon 2$ allele frequency was lower than in the control group ($\chi^2 = 10.6$, $P = 0.005$, LR 12.7), the $\epsilon 3$ allele frequency was lower than the bvFTD group ($\chi^2 = 6.2$, $P = 0.044$, LR 7.6), and the $\epsilon 4$ allele frequency was higher than in the control group ($\chi^2 = 20.3$, $P < 0.001$, LR 22.2) and the bvFTD group ($\chi^2 = 9.3$, $P = 0.010$, LR 10.7). The apoE allele frequencies did not significantly differ between the bvFTD group and the control group.

Table 2 reports main demographic, clinical characteristics of apoE $\epsilon 4$ carriers and noncarriers, stratified by diagnosis. There were no differences in age, gender, education, or disease severity [clinical dementia rating (CDR), CDR box, and mini mental state examination (MMSE)] between carriers and noncarriers within each group. Neuropsychological testing results for apoE $\epsilon 4$ carriers and noncarriers, stratified by diagnosis, are shown in Table S1. No significant differences were found in these measures between $\epsilon 4$ carriers and noncarriers in any of the groups.

Neuroimaging. The aim of our neuroimaging investigation was to evaluate whether $\epsilon 4$ influences brain morphology in non-Alzheimer's dementia, and, if so, whether the effect follows an AD-pattern of atrophy or whether the $\epsilon 4$ effect is found in regions typically involved in bvFTD.

We first searched for any regions where presence or absence of $\epsilon 4$ influences GM atrophy in similar regions across all diagnostic groups. No significant regions of atrophy shared by AD and bvFTD carriers or noncarriers were found. We then moved to investigate the effect of genotype on areas typical of each disease.

AD. We identified GM regions specifically atrophied in AD $\epsilon 4$ carriers relative to both AD $\epsilon 4$ noncarriers and controls (Fig. 1 and Table S2; see Methods for contrast details). These GM regions included the bilateral parietal cortex and the right precuneus, hippocampus, and middle frontal gyrus. These areas are included in the anatomical network typically involved in studies of path-proven AD (23) and in our AD patient sample, when considering all patients vs. controls. Fig. 1 illustrates this point by showing thresholded statistical maps of areas more involved for AD $\epsilon 4$ carriers vs. noncarriers superimposed (in red) on the regions that were more atrophied in all AD patients vs. controls (in yellow). When contrasting AD $\epsilon 4$ noncarriers with both $\epsilon 4$ carriers and controls, no areas of greater GM atrophy were observed.

bvFTD. When assessing regions of significant GM atrophy in bvFTD $\epsilon 4$ carriers relative to both bvFTD $\epsilon 4$ noncarriers and controls (Fig. 2 and Table S2), we identified the anterior insula, anterior cingulate cortex bilaterally, a broad area in the right frontal cortex comprising the superior and middle frontal gyri, supplementary motor area, superior orbitofrontal gyri, and middle cingulate cortex. Additional small regions of GM atrophy were also observed in the right caudate, superior temporal gyrus, and left superior, middle, inferior, superior- and inferior-orbital frontal gyri. As in the case of AD, differential atrophy between bvFTD $\epsilon 4$ carriers and noncarriers occurred in anatomical regions described as typical for bvFTD in studies of path-proven cases (23) and in our bvFTD cohort. Fig. 2 illustrates this point by showing that statistical maps of areas more involved for bvFTD $\epsilon 4$ carriers vs. noncarriers and controls (in blue) are superimposed on the overall regions that were atrophied in all bvFTD cases vs. controls (in cyan). When contrasting bvFTD $\epsilon 4$ noncarriers with both $\epsilon 4$ carriers and controls, no areas of greater GM atrophy were found.

Discussion

This study evaluated the effect of apoE $\epsilon 4$ on cognitive and neuroimaging features in a well-characterized cohort of patients with neurodegenerative disease of different etiologies. ApoE4

Table 2. Main demographic and clinical characteristics of apoE $\epsilon 4$ carriers and noncarriers, stratified by diagnostic group

Subjects (n)	AD		bvFTD		Controls	
	$\epsilon 4-$ (21)	$\epsilon 4+$ (30)	$\epsilon 4-$ (23)	$\epsilon 4+$ (8)	$\epsilon 4-$ (46)	$\epsilon 4+$ (10)
Mean age (SD), years	67.9 (11.2)	66.5 (10.7)	58.4 (10.9)	58.9 (4.3)	66.5 (9.4)	66.9 (7.6)
Women/Men	14/7	13/17	7/16	3/5	27/19	5/5
Mean education (SD), years	15.1 (3.4)	15.4 (3.3)	16.0 (2.4)	15.8 (2.5)	17.5 (1.8)	18.6 (2.7)
Mean MMSE (SD)	21.6 (4.4)	21.5 (6.2)	22.7 (7.0)	22.0 (7.8)	29.6 (0.6)	29.7 (0.7)
Median CDR total (range)	1.0 (0.5–2)	1.0 (0.5–2)	1.0 (0.5–3)	1.0 (0.5–2)	0.0 (NA)	0.0 (NA)
Median CDR box score (range)	5.0 (1.5–10)	4.8 (2–12)	8.0 (2.5–15)	7.3 (4–8.5)	0.0 (0–0.5)	0.0 (0–0.5)

Comparisons between $\epsilon 4$ carriers and noncarriers within each diagnostic group were performed by using the Pearson χ^2 test for gender and CDR, and Kruskal-Wallis one-way ANOVA by ranks test for age, education, and CDR box score. No significant differences were found between $\epsilon 4$ carriers and noncarriers within any of the groups. NA, not applicable.

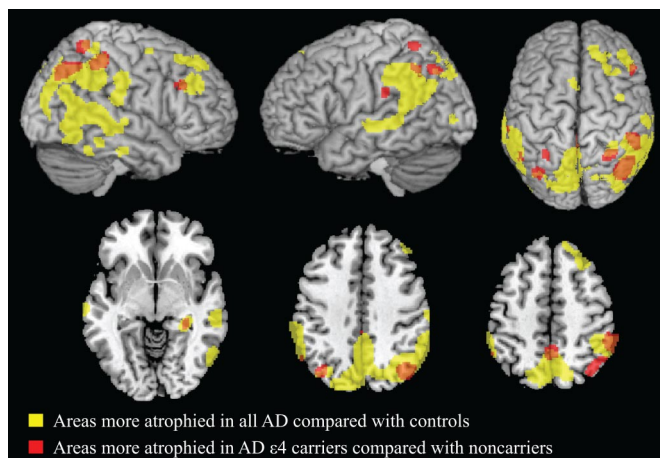


Fig. 1. Regions of GM atrophy in all AD patients compared with controls are shown in yellow. GM regions more atrophied in AD patients carrying apoE ϵ 4 relative to both AD noncarriers and controls are superimposed in red. Overlapping regions are shown in orange. AD ϵ 4 carriers had more GM atrophy than AD noncarriers in the bilateral parietal cortex and in the right hippocampus, precuneus, and middle frontal gyrus. Results are shown on the 3D rendering and axial sections of the Montreal Neurological Institute standard brain in neurological convention, and displayed at the threshold specified in *Materials and Methods*.

was associated with a more severe disease-specific pattern of brain atrophy in patients with probable AD and bvFTD at presentation. However, no significant differences were observed in cognitive profiles between ϵ 4 carriers and noncarriers in either of the disease groups. This disease-specific regional ϵ 4 effect is consistent with the hypothesis that apoE4 may affect the morphologic expression uniquely in different neurodegenerative diseases.

In AD, we found the strongest ϵ 4 effect in neocortical regions, particularly in bilateral inferior parietal cortex but also in the precuneus and right dorsolateral prefrontal cortex. One possible explanation for this finding in our study is the inclusion of early

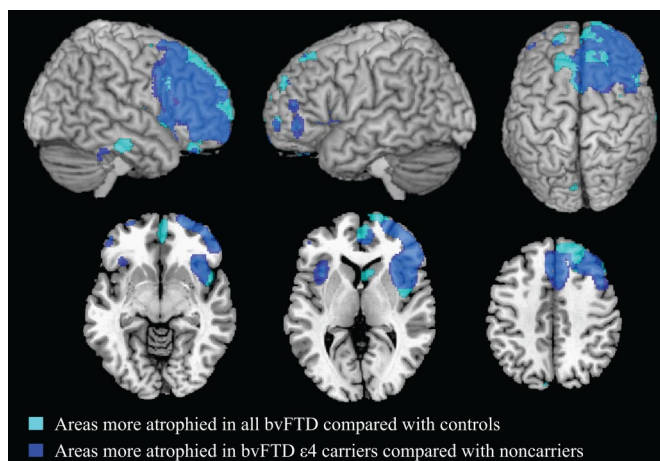


Fig. 2. Regions of GM atrophy in all bvFTD patients compared with controls are shown in cyan. GM regions more atrophied in bvFTD patients carrying apoE ϵ 4 relative to both bvFTD noncarriers and controls are superimposed in blue. Overlapping regions are shown in light blue. bvFTD ϵ 4 carriers had more GM atrophy than bvFTD noncarriers in the bilateral medial, dorsolateral, orbital frontal cortex, anterior insula, and cingulate cortex with right predominance. Results are shown on the 3D rendering and axial sections of the Montreal Neurological Institute standard brain in neurological convention and displayed at the threshold specified in *Materials and Methods*.

age-of-onset AD (age of onset below 65) because these same neocortical regions coincide with areas most severely affected in younger AD patients (24). AD ϵ 4 carriers also had more hippocampal atrophy than noncarriers, which is consistent with the majority of existing *in vivo* neuroimaging studies (19–21). Although this was not a longitudinal study, apoE ϵ 4 dose has also been correlated with the rate of hippocampal atrophy (25). When considering the effect of apoE4 on AD pathology, ϵ 4 carriers have more senile plaques than noncarriers (14).

In bvFTD, the ϵ 4 allele influenced GM atrophy in a specific subset of frontal and insular regions, predominately in the right hemisphere. These regions fall within the atrophy pattern typically seen in bvFTD (26). Interestingly, within these same right-sided areas of ϵ 4 effect are the regions recently identified as the sites of earliest injury in bvFTD (27) and associated with more severe behavioral impairments in dementia (26). A regional-specific ϵ 4 effect in bvFTD was also proposed by a small exploratory study that showed a trend of greater atrophy in the ventral striatum and right frontotemporal regions in two bvFTD ϵ 4 carriers relative to six noncarriers (21). The only available study that looked at the clinical effect of apoE4 in FTD showed more severe behavioral disturbances in ϵ 4 carriers vs. noncarriers (18). Similarly, we recently observed two first-degree relatives with familial FTD-motor neuron disease who had dramatically different clinical presentations; the patient who was homozygous ϵ 4/ ϵ 4 presented with more profound cognitive and behavioral changes than his sibling who was homozygous ϵ 3/ ϵ 3 (28). One may speculate that these observed behavioral changes associated with ϵ 4 were due to the involvement of similar brain regions to those we found more atrophied in ϵ 4 carriers. The findings of the present study, when considered together with these previous observations, suggest that apoE4 may influence the pathology of bvFTD.

The pathological role of apoE4 in the CNS is mostly based on AD models, where both A β -dependent and independent mechanisms have been proposed (1). Through A β -independent pathways (1), apoE4 may contribute to neurodegenerative diseases other than AD. One such mechanism is the “two-hit” hypothesis (13, 29). In response to stressors or injury (“first hit”), neurons begin to synthesize apoE (1, 29). Although apoE may promote neuronal repair (2, 29), it can also undergo proteolytic cleavage. Carboxyl-terminal-truncated apoE fragments may disrupt the cytoskeleton, stimulate tau phosphorylation, impair mitochondrial function, and ultimately cause cell death (“second hit”) (29). The apoE4 isoform may have the most detrimental effect because it is more susceptible to proteolytic cleavage than E3 or E2 (1). This “two hit” phenomenon may be particularly relevant to our neuroimaging findings because of the unique, disease-specific, neural networks that were most severely atrophied in association with ϵ 4 carrier status. Under this paradigm, these same diseased regions are the initial sites of injury (“first hit”) and are particularly vulnerable in the presence of apoE4 fragments (“second hit”). ApoE4 influences both disease risk and brain atrophy in AD but only brain atrophy in bvFTD; this finding further highlights the different molecular mechanisms that may involve apoE4 in neurodegenerative disease. Clearly, apoE4 effects may occur either upstream or downstream of the initial “hit”.

In the present study, the more severe pattern of brain atrophy in ϵ 4 carriers did not correlate with the severity of cognitive impairment at presentation in any of the diagnostic groups. In AD patients, this finding agrees with the available literature, showing an inconsistent effect of apoE genotype on clinical severity at presentation (30, 31). The majority of longitudinal studies, although, have shown that ϵ 4 is associated with more rapid cognitive decline in AD (4). One may postulate that the higher risk for cognitive decline in AD ϵ 4 carriers may, in fact, be associated with the more severe brain atrophy found early in

the disease. In bvFTD, no studies have assessed the effects of apoE4 on cognitive measures such as we studied. However, one study that characterized a cohort of FTD patients with progranulin (PGRN) mutations found that $\epsilon 4$ carriers complained of earlier memory impairment than noncarriers (32). Clearly, longitudinal studies are needed to assess whether $\epsilon 4$ carrier status may influence disease progression, as has been shown in AD. Certainly, the atrophy patterns in our VBM study suggest that the FTD $\epsilon 4$ carriers may be at higher risk for rapid clinical decline.

This study is not without limitations. First, the sample sizes may have been insufficient to detect small differences in cognitive measures within each diagnostic group. Second, a vast majority of our cases are not pathology-confirmed; however, these patients were well characterized by a multidisciplinary team, and the accuracy of the clinical diagnoses was supported in all cases that underwent 11C-labeled Pittsburgh Compound-B (11C-PIB) PET imaging or that came to autopsy. The autopsy results on the available five bvFTD cases highlight the pathological heterogeneity of FTLT with Pick's disease, progressive supranuclear palsy (PSP), and corticobasal degeneration (CBD), all falling within the FTLT spectrum of disease (33), and additional AD features present in one case. Finally, although we performed extensive neuropsychological testing, no quantitative social-behavioral measures are available to fully characterize FTD patients.

This study shows that apoE4 not only influences brain morphology in AD but also has an effect in another neurodegenerative disease. Remarkably, the $\epsilon 4$ effect is restricted to disease-specific regions in both disorders. Understanding the role of apoE4 as a potential causative factor in neurodegeneration is especially appealing because therapies that target the structure and function of apoE are under investigation. To confirm whether our findings of $\epsilon 4$ effects in vulnerable neural networks are clinically meaningful, larger studies are needed to investigate the association of $\epsilon 4$ on clinical progression in FTLT-spectrum disorders.

Materials and Methods

Patient Selection. We searched the University of California, San Francisco Memory and Aging Center (UCSF MAC) database for all patients with known apoE genotypes who were seen between 1999 and 2007. From this group, we selected patients with clinical diagnoses of AD, bvFTD, and healthy controls. These diagnoses were derived by a multidisciplinary team consisting of neurologists, neuropsychologists, and psychiatrists who performed extensive behavioral, neuropsychological, and neuroimaging assessments. Patients who did not meet standard research criteria for probable AD National Institute of Neurological and Communicative Disorders and Stroke-Alzheimer's Disease and Related Disorders Association (NINCDS-ADRA) (34) or bvFTD (35) were excluded. During the selection process, neuroimaging findings were used only to exclude other causes of focal or diffuse brain damage, including extensive white matter disease.

From this cohort, we excluded two AD patients who had presenilin1 (PSEN1) mutations of four AD patients screened for PSEN1, three bvFTD patients with PGRN mutations of 31 bvFTD screened for PGRN, and one control subject who was a blood relative of a patient with a PGRN mutation because of reports that these genetic mutations may influence brain morphology (36, 37). In addition, no microtubule associated protein tau (MAPT) mutations were found in the 14 bvFTD patients screened for MAPT. Then, we excluded one AD and three bvFTD cases because poor image quality precluded proper brain segmentation in Statistical Parametric Mapping (SPM5).

We included 51 patients with AD (age 51 to 86), 31 patients with bvFTD (age 29 to 80), and 56 healthy controls (age 38 to 82). Autopsies were performed on available cases at the University of Pennsylvania or at UCSF by using a published protocol (38); no cases were excluded based on autopsy results. Three patients in the AD group came to autopsy, and all met pathologic criteria for moderate-to-high likelihood AD (NIA-Reagan) (39); one of these cases had additional Lewy body pathology. Of the five bvFTD cases that came to autopsy, the pathological diagnoses were as follows: Pick's disease (two cases) (40), "tauopathy" with features of FTLT and PSP, PSP comorbid with AD, and CBD. Seven AD and three bvFTD patients underwent 11C-PIB PET imaging to assess

for evidence of amyloid deposition by using a described protocol (41). Distribution volume ratio images (cerebellar reference) were visually assessed by two investigators blinded to clinical diagnosis, and scans were read as positive or negative for cortical 11C-PIB uptake. In agreement with their clinical diagnoses, all seven AD cases were PIB-positive and all three bvFTD cases were PIB-negative. This study was approved by the UCSF and University of Pennsylvania committees on human research. All subjects provided written informed consent before participating.

Genetic Analysis. *ApoE.* DNA was purified from peripheral blood samples (Gentra PureGene Blood Kit, Qiagen) by using the recommended protocol. Primers GCATCTGCTCTGCATCTGTC (forward) and ACCTGCTCCTCAC-CTGTC (reverse) were chosen to straddle a 687-bp region spanning the $\epsilon 4$ and $\epsilon 2$ polymorphisms. Genomic DNA was amplified by standard PCR methods, labeled, and sequenced by using a 3730 XL ABI Prism. Polymorphism calls were performed by Sequencher (GeneCodes) and manually confirmed for accuracy. *PSEN1.* Primer pairs complementary to the intronic regions of PSEN1 were used to amplify exon 3–12. Both strands of the PCR products were sequenced by using the CEQ dye terminator cycle sequencing kit on a CEQ 8000 using both the forward and reverse PCR primers. If a mutation was identified, confirmatory sequencing was performed. Sequence analysis was performed with Sequencher software.

MAPT. DNA was isolated from peripheral blood. Primer pairs complementary to the intronic regions of tau were used to amplify exons 1–5, 7, and 9–13. Both strands of the PCR products were sequenced. Sequence analysis was performed with Sequencher software.

PGRN. DNA was sent from a stored sample. All 12 coding exons of PGRN and the noncoding exon 0 were amplified from genomic DNA by PCR using primers designed to flank intronic sequence.

Cognitive Assessment. The neuropsychological measures included in our bedside screening protocol have been described in ref. 26. Briefly, general intellectual functioning was assessed with the MMSE whereas global functional assessment was evaluated by using CDR. Verbal episodic memory was evaluated by using the California Verbal Learning Test - Short Form (CVLT-SF) and visual-nonverbal episodic memory was measured with the 10-min free recall of modified Rey-Osterrieth (Rey-O) complex figure. Copy of the modified Rey-O assessed visuospatial functioning. Language assessment included the abbreviated (15 item) Boston Naming Test and semantic fluency (animals generated in 1 min). Tests of executive functioning included a modified version of the Trails B test (correct lines in 120 s), maximum backward digit span, and phonemic fluency (D-words generated in 1 min).

Statistical Analysis. Differences among the groups in apoE genotypes and allele frequencies were tested by using the Pearson χ^2 test; all probability (P) values <0.05 are reported. Differences between apoE4 carriers and noncarriers within each diagnostic group were performed by using the Pearson χ^2 test for gender and CDR, and Kruskal-Wallis one-way ANOVA by ranks test for age, education, CDR box score, MMSE, and neuropsychological measures. Post hoc analysis included Bonferroni correction for multiple pairwise comparisons, and a P value <0.01 was considered significant. Statistical analyses were performed with SPSS software version 16.0 for Windows.

MRI Study. MRI scans were obtained on a 1.5 Tesla Magnetom VISION system (Siemens). Structural MRI sequences included the following: (i) double spin echo sequence [repetition time (TR) = 5000 ms, echo time (TE) = 20/80 ms, 51 contiguous axial slices, thickness = 3 mm, 1.0×1.25 mm² in-plane resolution] and (ii) volumetric magnetization prepared rapid gradient echo sequence (TR = 10 ms, TE = 4 ms, inversion time = 300 ms, flip angle = 15°, coronal orientation perpendicular to the double echo sequence, matrix size = 256×192 , voxel resolution = $1.0 \times 1.0 \times 1.0$ mm, slab thickness = 1.5 mm). VBM analysis includes two steps: spatial preprocessing (normalization, segmentation, Jacobian modulation, and smoothing) and statistical analysis (22). Both stages were performed by using the SPM5 software package (Wellcome Department of Imaging Neuroscience) running on Matlab 7.0.1 (Math Works). MRI images were segmented, normalized, and modulated by using the unified segmentation model (42). This model also includes parameters that account for image intensity nonuniformity. To help remove nonbrain tissue, the "clean-up" procedure was applied to the segmented GM images. The final voxel resolution after normalization was $2.0 \times 2.0 \times 2.0$ mm. Spatially normalized, modulated GM images were then smoothed with a 12-mm FWHM isotropic Gaussian kernel.

Age, gender, disease severity (CDR box score), and total intracranial volume were entered into the design matrix as nuisance variables. Regionally specific differences in GM volumes were assessed by using the general linear model

and the significance of each effect was determined by using the theory of Gaussian fields (43). We first searched for areas of greater GM atrophy in $\epsilon 4$ carriers vs. noncarriers within healthy controls at the lowest threshold ($P < 0.001$, uncorrected for multiple comparisons), and no significant regions were identified. Thus, healthy controls were considered as a unique group for all following comparisons.

First, direct comparisons were performed to identify GM atrophy in all AD and all bvFTD patients vs. controls, and GM regions more atrophied within each apoE $\epsilon 4$ carriers and noncarriers group vs. controls. To investigate whether apoE $\epsilon 4$ has a similar influence on brain morphology regardless of diagnostic group, the following contrasts were performed: (i) all (AD and bvFTD) $\epsilon 4$ carriers vs. controls contrast inclusively masked by $\epsilon 4$ carriers vs. noncarriers contrast within each diagnostic group (i.e., AD carriers vs. noncarriers and bvFTD carriers vs. noncarriers); the inclusive masking procedure limits the main effect contrast to regions that are also present in carriers vs. controls contrast; and (ii) all $\epsilon 4$ noncarriers vs. controls contrast inclusively masked by the noncarriers vs. carriers contrast within each diagnostic group. Then, specific contrasts were performed to investigate the GM regions more atrophied in $\epsilon 4$ carriers vs. noncarriers and vice versa in each diagnostic group

- Mahley RW, Weisgraber KH, Huang Y (2006) Apolipoprotein E4: A causative factor and therapeutic target in neuropathology, including Alzheimer's disease. *Proc Natl Acad Sci USA* 103:5644–5651.
- Mahley RW (1988) Apolipoprotein E: Cholesterol transport protein with expanding role in cell biology. *Science* 240:622–630.
- Farrer LA, et al. (1997) Effects of age, sex, and ethnicity on the association between apolipoprotein E genotype and Alzheimer disease. A meta-analysis. *APOE and Alzheimer Disease Meta Analysis Consortium Jama* 278:1349–1356.
- Cosentino S, et al. (2008) APOE epsilon 4 allele predicts faster cognitive decline in mild Alzheimer disease. *Neurology* 70:1842–1849.
- Schultz MR, et al. (2008) Apolipoprotein E genotype and memory in the sixth decade of life. *Neurology* 70:1771–1777.
- Ariza M, et al. (2006) Influence of APOE polymorphism on cognitive and behavioural outcome in moderate and severe traumatic brain injury. *J Neurol Neurosurg Psychiatry* 77:1191–1193.
- Louko AM, Vilkki J, Niskakangas T (2006) ApoE genotype and cognition after subarachnoid haemorrhage: A longitudinal study. *Acta Neurol Scand* 114:315–319.
- Tian J, et al. (2004) Association between apolipoprotein E $\epsilon 4$ allele and arteriosclerosis, cerebral amyloid angiopathy, and cerebral white matter damage in Alzheimer's disease. *J Neurol Neurosurg Psychiatry* 75:696–699.
- Li YJ, et al. (2004) Apolipoprotein E controls the risk and age at onset of Parkinson disease. *Neurology* 62:2005–2009.
- Tsuang DW, et al. (2002) Familial dementia with lewy bodies: A clinical and neuropathological study of 2 families. *Arch Neurol* 59:1622–1630.
- Li YJ, et al. (2004) Apolipoprotein E is associated with age at onset of amyotrophic lateral sclerosis. *Neurogenetics* 5:209–213.
- Holtzman DM, et al. (2000) Apolipoprotein E isoform-dependent amyloid deposition and neuritic degeneration in a mouse model of Alzheimer's disease. *Proc Natl Acad Sci USA* 97:2892–2897.
- Mahley RW, Huang Y (2006) Apolipoprotein (apo) E4 and Alzheimer's disease: Unique conformational and biophysical properties of apoE4 can modulate neuropathology. *Acta Neurol Scand Suppl* 185:8–14.
- Gomez-Isla T, et al. (1996) Clinical and pathological correlates of apolipoprotein E epsilon 4 in Alzheimer's disease. *Ann Neurol* 39:62–70.
- Bernardi L, et al. (2006) The effects of APOE and tau gene variability on risk of frontotemporal dementia. *Neurobiol Aging* 27:702–709.
- Riemenschneider M, Diehl J, Muller U, Forstl H, Kurz A (2002) Apolipoprotein E polymorphism in German patients with frontotemporal degeneration. *J Neurol Neurosurg Psychiatry* 72:639–641.
- Srinivasan R, et al. (2006) The apolipoprotein E epsilon4 allele selectively increases the risk of frontotemporal lobar degeneration in males. *J Neurol Neurosurg Psychiatry* 77:154–158.
- Engelborghs S, et al. (2006) Dose dependent effect of APOE epsilon4 on behavioral symptoms in frontal lobe dementia. *Neurobiol Aging* 27:285–292.
- Lehtovirta M, et al. (1995) Volumes of hippocampus, amygdala and frontal lobe in Alzheimer patients with different apolipoprotein E genotypes. *Neuroscience* 67:65–72.
- Geroldi C, et al. (2000) Apolipoprotein E genotype and hippocampal asymmetry in Alzheimer's disease: A volumetric MRI study. *J Neurol Neurosurg Psychiatry* 68:93–96.
- Boccardi M, et al. (2004) APOE and modulation of Alzheimer's and frontotemporal dementia. *Neurosci Lett* 356:167–170.
- Good CD, et al. (2002) Automatic differentiation of anatomical patterns in the human brain: Validation with studies of degenerative dementias. *Neuroimage* 17:29–46.
- Rabinovici GD, et al. (2007) Distinct MRI atrophy patterns in autopsy-proven Alzheimer's disease and frontotemporal lobar degeneration. *Am J Alzheimer's Dis Other Demen* 22:474–488.
- Frisoni GB, et al. (2007) The topography of grey matter involvement in early and late onset Alzheimer's disease. *Brain* 130:720–730.
- Mori E, et al. (2002) Accelerated hippocampal atrophy in Alzheimer's disease with apolipoprotein E epsilon4 allele. *Ann Neurol* 51:209–214.
- Rosen HJ, et al. (2002) Patterns of brain atrophy in frontotemporal dementia and semantic dementia. *Neurology* 58:198–208.
- Seeley WW, et al. (2008) Frontal paralimbic network atrophy in very mild behavioral variant frontotemporal dementia. *Arch Neurol* 65:249–255.
- Vossel K, et al. (2008) Clinicopathological case comparison: Familial frontotemporal lobar degeneration-motor neuron disease with phenotypic heterogeneity in two first-degree relatives. *Neurology* 70(Suppl 1):A275.
- Xu Q, et al. (2008) Intron-3 retention/splicing controls neuronal expression of apolipoprotein E in the CNS. *J Neurosci* 28:1452–1459.
- Marra C, et al. (2004) Apolipoprotein E epsilon4 allele differently affects the patterns of neuropsychological presentation in early- and late-onset Alzheimer's disease patients. *Dement Geriatr Cogn Disord* 18:125–131.
- Snowden JS, et al. (2007) Cognitive phenotypes in Alzheimer's disease and genetic risk. *Cortex* 43:835–845.
- Rademakers R, et al. (2007) Phenotypic variability associated with progranulin haploinsufficiency in patients with the common 147C>T (Arg493X) mutation: An international initiative. *Lancet Neurol* 6:857–868.
- Sha S, Hou C, Viskontas IV, Miller BL (2006) Are frontotemporal lobar degeneration, progressive supranuclear palsy and corticobasal degeneration distinct diseases? *Nat Clin Pract Neurol* 2:658–665.
- McKhann G, et al. (1984) Clinical diagnosis of Alzheimer's disease: Report of the NINCDS-ADRDA Work Group under the auspices of Department of Health and Human Services Task Force on Alzheimer's Disease. *Neurology* 34:939–944.
- Neary D, et al. (1998) Frontotemporal lobar degeneration: A consensus on clinical diagnostic criteria. *Neurology* 51:1546–1554.
- Beck J, et al. (2008) A distinct clinical, neuropsychological and radiological phenotype is associated with progranulin gene mutations in a large UK series. *Brain* 131:706–720.
- Gregory GC, Macdonald V, Schofield PR, Kril JJ, Halliday GM (2006) Differences in regional brain atrophy in genetic forms of Alzheimer's disease. *Neurobiol Aging* 27:387–393.
- Forman MS, et al. (2006) Frontotemporal dementia: Clinicopathological correlations. *Ann Neurol* 59:952–962.
- The National Institute on Aging and Reagan Institute Working Group on Diagnostic Criteria for the Neuropathological Assessment of Alzheimer's Disease. (1997) Consensus recommendations for the postmortem diagnosis of Alzheimer's disease. *Neurobiol Aging* 18:S1–2.
- McKhann GM, et al. (2001) Clinical and pathological diagnosis of frontotemporal dementia: Report of the Work Group on Frontotemporal Dementia and Pick's Disease. *Arch Neurol* 58:1803–1809.
- Rabinovici GD, et al. (2007) 11C-PIB PET imaging in Alzheimer disease and frontotemporal lobar degeneration. *Neurology* 68:1205–1212.
- Ashburner J, Friston KJ (2005) Unified segmentation. *Neuroimage* 26:839–851.
- Friston KJ, et al. (1995) Analysis of fMRI time-series revisited. *Neuroimage* 2:45–53.

(AD and bvFTD). Specifically, the following contrasts were performed: (i) disease group $\epsilon 4$ carriers vs. controls contrast inclusively masked by the carriers vs. noncarriers contrast within each diagnostic group, and (ii) disease group $\epsilon 4$ noncarriers vs. controls contrast inclusively masked by the noncarriers vs. carriers contrast within each diagnostic group. A level of significance of $P < 0.05$ corrected for multiple comparisons (family-wise error) was accepted for the main contrasts that compared patients to controls and of $P < 0.05$ uncorrected for the masks that entailed within group comparisons.

ACKNOWLEDGMENTS. We thank Gil D. Rabinovici and William J. Jagust for PIB imaging, William W. Seeley for help in selecting patients, and John Neuhaus for assistance with statistics. We also thank all of the study participants and their families for their support to our research. This study was supported by the National Institutes of Health Grants R01 NS050915, P50 AG03006, P01 AG019724, K23 NS408855, and R01 AG022983; State of California Grant Department of Health Services (DHS) 04–35516; Alzheimer's Disease Research Center of California (ARCC) Grant 03–75271 DHS/Alzheimer's Disease Program (ADP)/ARCC; John Douglas French Alzheimer's Foundation; Alzheimer's Association Grant NIRG-07–59422; the Larry L. Hillblom Foundation; the Koret Family Foundation; and the McBean Family Foundation. PIB-PET scans were supported by National Institute on Aging Grant AG027859.